

Structural selective charge transfer in iodine-doped carbon nanotubes

**T. Michel, L. Alvarez, J.-L. Sauvajol, R. Almairac, R. Aznar, O. Mathon,
J.-L. Bantignies and E. Flahaut**

LCVN, Université Montpellier 2, UMR 5587, 34095 Montpellier cedex 05, France

ESRF, Rue Jules Horowitz, BP 220, 38043, Grenoble Cedex, France

Centre Interuniversitaire de Recherche et d'ingénierie des matériaux (IMR CNRS 5085),

Iniversité Paul Sabatier, 31602 Toulouse Cedex 4, France

Abstract

We have investigated iodine intercalated carbon nanostructures by extended X-ray absorption fine structure (EXAFS) and Raman spectroscopies. We discuss here the charge transfer and the iodine–carbon interaction as a function of the carbon nanostructures (graphite, multi-walled, double-walled and single walled nanotubes). The results show that iodine is weakly adsorbed on the surface of all multi-walled nanotubes. By contrast, a charge transfer between iodine and single walled nanotubes is evidenced.

Keywords: A. Nanostructures; C. XAFS

1. Introduction
 2. Experimental
 - 2.1. Samples
 - 2.2. Experimental set-up
 - 2.3. Data analysis
 3. Results
 4. Conclusion
- References

1. Introduction

The electronic properties of carbon nanostructures can be controlled by intercalation of guest species to form compounds analogous to graphite intercalation compounds [1]. Single-wall carbon nanotubes (SWNTs) can be doped with either donors (K, Rb...) or acceptors (Br₂, I₂) [2]. Iodine intercalation of multi-walled carbon nanotubes (MWNTs) is not clearly understood. Indeed, the low frequency range of the Raman spectra displays two new peaks around 110 and 170 cm⁻¹, assigned to the presence of iodine chains (In)⁻ [3] and [4]. The ionic form of the iodine chain is consistent with a charge transfer [4]. However, the high frequency modes are not affected by the incorporation of the iodine species, so that no clear evidence of the charge transfer in iodine doped MWNTs (I-MWNTs) can be obtained from Raman spectroscopy [4].

In the case of iodine doped SWNT (I-SWNTs), previous works mainly focus their study on the iodine localization within the bundle [3], [4], [5] and [6]. However, to our knowledge, the structure of the intercalated iodine anion chain is still not unambiguously determined.

In this paper, we report an EXAFS investigation combined with a Raman study in order to discuss the interaction between iodine and several nanostructures such as graphite, multi-walled nanotubes (I-MWNTs), double-walled nanotubes (I-DWNTs) and single-walled nanotubes (I-SWNTs). Graphite, MWNTs and DWNTs will be named layered carbon solids (LCS).

2. Experimental

2.1. Samples

Commercial HIPCO SWNT [7] are studied. In all cases, the raw materials are characterized by X-ray diffraction and selected using the strength of the (10) reflection of the bundles. Consequently, the sample we study contains a large amount of bundles. MWNTs are synthesized by CVD method [8].

After outgassing and annealing the selected samples at 250 °C for 24 h under dynamical vacuum, iodine doping of the carbon materials is achieved by immersing the nanomaterials in molten iodine in an evacuated quartz tubes at a temperature $T=140$ °C for several days to perform a saturation doping [3]. The excess of iodine is removed by the cold point method.

After doping, materials are separated into two parts. We use a reference set of materials and a second set of carbon materials washed by ethanol several times in order to remove the iodine species weakly adsorbed at the surface of the materials and I₂ crystallites mixed with the doped nanotube powder.

2.2. Experimental set-up

Low temperature (10 K) XAS experiments are performed at the beamline BM 29 at ESRF facility. Spectra were measured at the iodine K-edge ($E_0=33.169$ keV) in the transmission mode with a double Si(311) crystals monochromator. Ionization chambers were used to detect the signals.

2.3. Data analysis

EXAFS oscillations $\chi(k)$ are extracted from XAS data using a standard procedure [9] and [10]. After the background subtraction and edge step normalization of the absorption data, the $\chi(k)$ signals are obtained. The pseudo radial function $FT(k\chi(k))$ is obtained by Fourier transform of $k\chi(k)$. Theoretical backscattering amplitudes, phases and mean free paths are obtained by FEFF calculations [11].

3. Results

Fig. 1 shows the EXAFS oscillations $k*\chi(k)$ of several unwashed iodine doped LCS and I-SWNTs. The spectra are very close to each other and display a good signal up to 15 \AA^{-1} . There are only small differences between I-SWNTs and the LCS marked by arrows on Fig. 1. For all the LCS, the Fourier Transforms $FT(k\chi(k))$ of all the spectra lead to very similar pseudo radial distribution (not shown). More precisely, three distinct neighbouring shells are observable up to 5 \AA , centred around 2.5 , 3.2 and 4.2 \AA as shown in Fig. 2 for I-MWNTs. By considering a cluster of I₂ molecules the EXAFS spectra are quite well reproduced by ab initio FEFF 8 calculations (Fig. 3). The $FT(k\chi(k))$ of the I-SWNTs samples is close to $FT(k\chi(k))$ of the I-MWNTs but cannot be simulated using the I₂ crystal structure. The latter result suggests that the intercalation processes are different in I-MWNTs and I-SWNTs respectively.

Fig. 1. EXAFS spectra $k^3\chi(k)$ of (a) Graphite, (b) I-MWNTs, (c) I-DWNTs and (d) I-SWNTs.

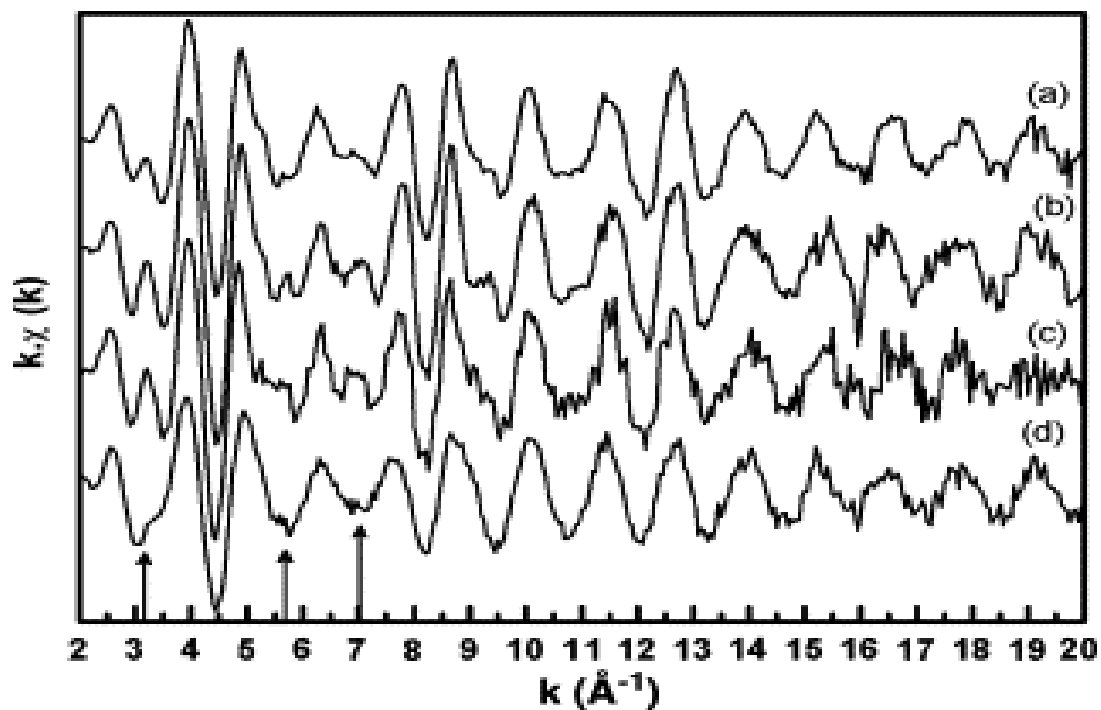


Fig. 2. Fourier Transform of the EXAFS spectra $k^3\chi(k)$ for raw MWNTs (topmost), raw SWNTs (middle) and washed I-SWNTs (bottommost).

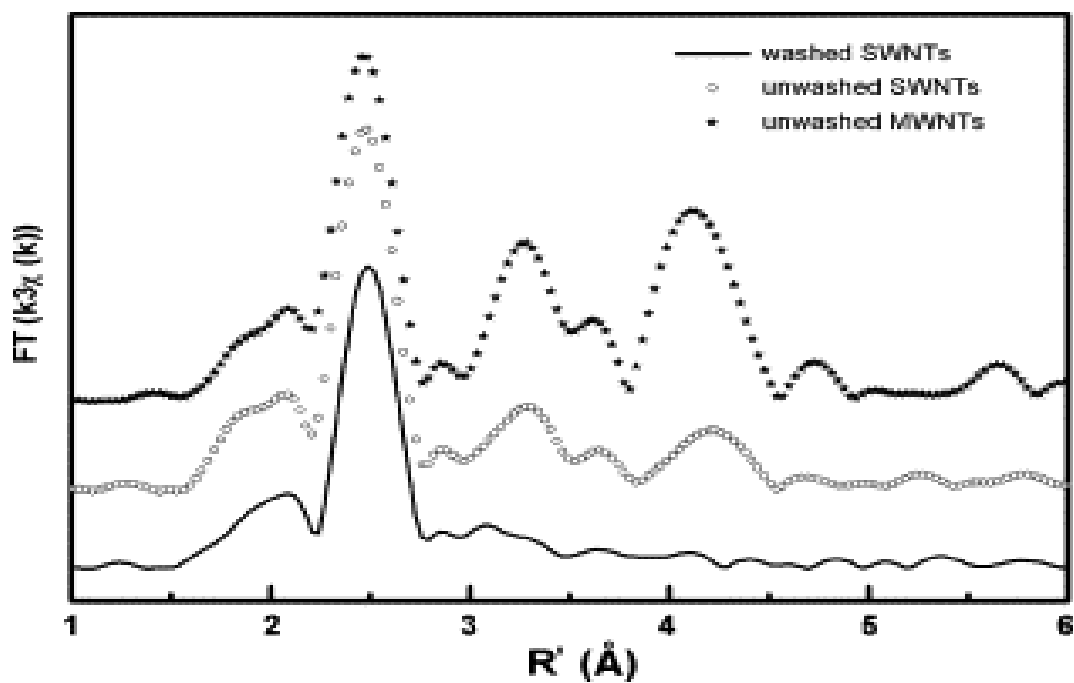
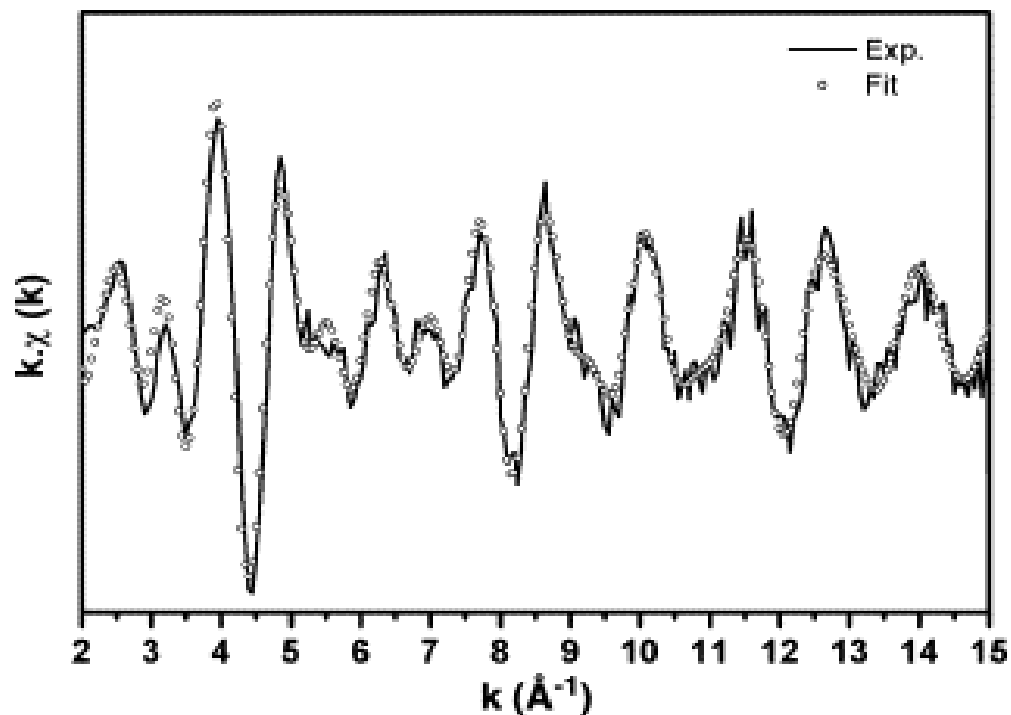


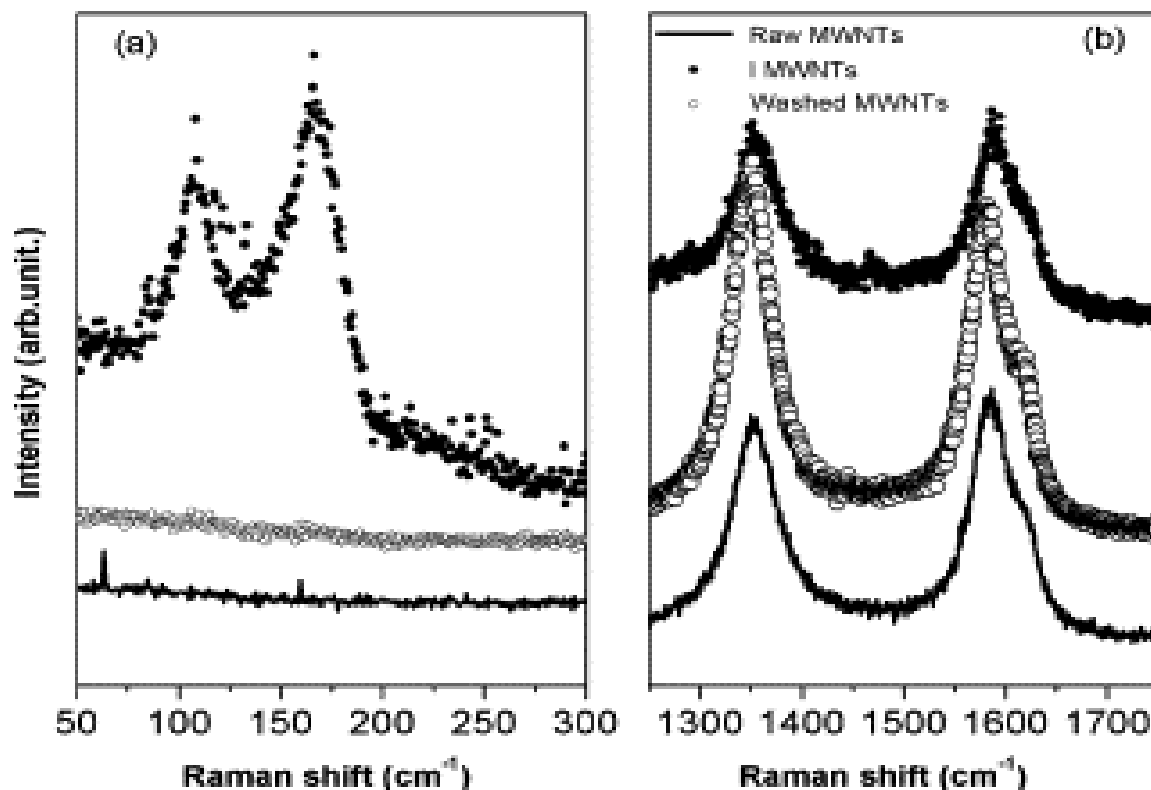
Fig. 3. Fourier Transform $FT(k^3 \chi(k))$ of raw MWNTs and its fit.



As the Raman spectra of all LCS are quite similar, [Fig. 4](#) only shows the spectra of the raw MWNTs, I-MWNTs and ethanol washed I-MWNTs. The peaks located, respectively, around 110 and 170 cm^{-1} ([Fig. 4a](#)) are generally attributed to the presence of $(\text{In})^-$ iodine chains. These anion chains are consistent with a charge transfer. However, unlike SWNTs, the tangential modes of LCS are not significantly affected by the presence of the iodine ([Fig. 4b](#)). To explain this discrepancy, it is generally assumed that in LCS, only the innermost surface (or the outermost) is intercalated, so that the Raman response in the graphite like modes region is dominated by non intercalated structures [4]. In addition, we assume that the neutral I_2 molecules signature (seen by EXAFS) is due to excessive iodine in our samples. To get rid of the iodine molecules at the surface of the samples, the samples are washed with ethanol. After that, it turns out that no absorption edge is observed on LCS, meaning that the interaction between iodine and the carbon network before washing is quite weak and that LCS compounds are not intercalated by iodine. By contrast, after washing, an iodine absorption edge is still observable on SWNTs samples (as shown in [Fig. 2](#), bottommost), meaning that iodine is still present in this type of carbon nanostructures. Thus, both EXAFS and Raman

results suggest that the iodine intercalation processes are different in LCS and SWNTs respectively.

Fig. 4. Raman spectra of raw MWNTs, I-MWNTs and washed I-MWNT. (a) in the low frequency range; (b) in the high frequency range.



To explain this result, we assume that two different interaction processes take place, respectively, in LCS compounds and in SWNTs. This assumption is consistent with thermogravimetric analysis (TGA) experiments for which different energies were required to remove iodine from MWNTs and SWNTs respectively. Indeed, the loss of iodine begins at room temperature for MWNT [4] and only at 100 °C for SWNT [3]. This difference can be explained considering distinct intercalation sites in I-MWNTs and I-SWNTs samples, the latter providing one specific site preventing iodine removing. Because of steric considerations, the interstitial site between three SWNTs within the bundles must be excluded. Indeed, according to the large van der Waals ionic iodine diameter ($\approx 4 \text{ \AA}$), penetration of iodine in the interstitial site has a low probability ($\approx 2.6 \text{ \AA}$ in diameter for (10,

10) SWNTs). In fact, to make all the results consistent, we assume that iodine species are localized outside MWNTs but can penetrate the inner cavity of SWNTs. Indeed, for DWNTs, only the outer tube is affected by the intercalation process [12]. The cap ends of SWNTs are probably much easier to open than those of MWNTs for which several layers have to be destroyed. Thus, iodine can penetrate SWNTs but not MWNTs.

4. Conclusion

To summarize, combining EXAFS and Raman experiments on iodine doped carbon nanostructures allowed us to evidence two different kinds of interactions between the iodine chains and the carbon network in I-MWNTs and I-SWNTs. We assume that those differences arise from different insertion sites of iodine within the samples, outside the LCS and inside the SWNTs, respectively.

References

- M.S. Dresselhaus and G. Dresselhaus, *Advanced Physics* **30** (1981), pp. 139–326.
- R.S. Lee, H.J. Kim, J.E. Fischer, A. Thess and R.E. Smalley, *Nature* **388** (1997), pp. 255–257.
- L. Grigorian, K.A. Williams, S. Fang, G.U. Sumanasekera, A.L. Loper, E.C. Dickey, S.J. Pennycook and P.C. Eklund, *Physical Review Letters* **80** (1998), pp. 5560–5563.
- W. Zhou, S. Xie, L. Sun, D. Tang, Y. Li, Z. Liu, L. Ci, X. Zou, G. Wang, P. Tan, X. Dong, B. Xu and B. Zhao, *Applied Physics Letters* **80** (2002), pp. 2553–2555.
- U.D. Venkateswaran, E.A. Brandsen, M.E. Katakowski, A. Harutyunyan, G. Chen, A.L. Loper and P.C. Eklund, *Physical Review B* **65** (2002), pp. 0541021–0541025.
- X. Fan, E.C. Dickey, P.C. Eklund, K.A. Williams, L. Grigorian, R. Buczko, S.T. Pantelides and S.J. Pennycook, *Physical Review Letters* **84** (2002), pp. 4621–4624.
- P. Nikolaev, M.J. Bronikowski, R.K. Bradley, F. Rohmund, D.T. Colbert, K.A. Smith and R.E. Smalley, *Chemical Physical Letters* **313** (1999), pp. 91–97.

E. Flahaut, A. Peigney, C. Laurent and A. Rousset, *Journal of Material Chemistry* **10** (2000), pp. 249–252.

D. Köningsberger and R. Prins, *X-ray Absorption Principles, Applications, Techniques of EXAFS, SEXAFS AND XANES*, Wiley (1988).

B.K. Teo, *EXAFS: Basic Principles and Data Analysis*, Springer, Berlin (1986).

A.L. Ankudinov, B. Ravel, J.J. Rehr, S.D. Conradson, *Physical Review B*, 58 (1998) 7565.

J. Cambedouzou, J.L. Sauvajol, A. Rahmani, E. Flahaut, A. Peigney, C. Laurent, *Physical Review B*, 69 (2004), 235422–1, 235422–6.

Original text : Elsevier.com